

# Crosstalk between neutrophils, B-1a cells and plasmacytoid dendritic cells initiates autoimmune diabetes

Julien Diana<sup>1,2,6</sup>, Yannick Simoni<sup>1,2,6</sup>, Laetitia Furio<sup>2,3,6</sup>, Lucie Beaudoin<sup>1,2</sup>, Birgitta Agerberth<sup>4</sup>, Franck Barrat<sup>5</sup> & Agnès Lehuen<sup>1,2</sup>

Type 1 diabetes develops over many years and is characterized ultimately by the destruction of insulin-producing pancreatic beta cells by autoreactive T cells. Nonetheless, the role of innate cells in the initiation of this disease remains poorly understood. Here, we show that in young female nonobese diabetic mice, physiological beta cell death induces the recruitment and activation of B-1a cells, neutrophils and plasmacytoid dendritic cells (pDCs) to the pancreas. Activated B-1a cells secrete IgGs specific for double-stranded DNA. IgGs activate neutrophils to release DNA-binding cathelicidin-related antimicrobial peptide (CRAMP), which binds self DNA. Then, self DNA, DNA-specific IgG and CRAMP peptide activate pDCs through the Toll-like receptor 9–myeloid differentiation factor 88 pathway, leading to interferon- $\alpha$  production in pancreatic islets. We further demonstrate through the use of depleting treatments that B-1a cells, neutrophils and IFN- $\alpha$ -producing pDCs are required for the initiation of the diabetogenic T cell response and type 1 diabetes development. These findings reveal that an innate immune cell crosstalk takes place in the pancreas of young NOD mice and leads to the initiation of T1D.

T cells infiltrate the pancreas and target insulin-producing beta cells during type 1 diabetes (T1D) development<sup>1</sup>. However, T cells represent only one piece of the puzzle of the multiple immune cells implicated in beta cell loss<sup>2</sup>. Plasmacytoid dendritic cells (pDCs) are central mediators of antiviral immunity through their ability to produce large amounts of interferon- $\alpha$  (IFN- $\alpha$ ) and IFN- $\beta$ <sup>3</sup>. In addition to their antiviral role, pDCs also promote various autoimmune diseases such as psoriasis and systemic lupus erythematosus (SLE)<sup>4,5</sup>. Regarding autoimmune diabetes, a pathogenic role for IFN- $\alpha$  and pDCs has been proposed, as IFN- $\alpha$  treatment of patients with viral infections or with leukemia has been shown to be associated with increased incidence of T1D<sup>6,7</sup>. Additionally, IFN- $\alpha$ -producing pDCs have been detected in the blood of patients with T1D at the time of diagnosis<sup>8</sup>. Furthermore, genetic analysis supports a diabetogenic role for IFN- $\alpha$ -induced genes in prediabetic children<sup>9</sup>. In mice, transgenic non-autoimmune-prone mice expressing IFN- $\alpha$  in beta cells develop autoimmune diabetes<sup>10</sup>. Subsequently, it was shown that IFN- $\beta$  accelerates the onset of the disease in nonobese diabetic (NOD) mice and breaks self tolerance to beta cell antigens in nonobese resistant mice<sup>11</sup>. This potential role of IFN- $\alpha$  and IFN- $\beta$  and pDCs in T1D and in other autoimmune diseases prompted us to investigate the functions of pDCs in the initiation of diabetes. It has been found that during the first postnatal weeks, waves of physiological beta cell death occur in rodents<sup>12–14</sup>, pigs<sup>15</sup> and humans<sup>16</sup>. Given that dead cell clearance is defective in NOD mice<sup>17</sup>, we speculate that the accumulation of beta cell debris (for example, self DNA) can activate pDCs in the pancreas.

## RESULTS

### Innate cells infiltrate the pancreas of young NOD mice

We initially focused on characterizing immune cell infiltration in the pancreas of NOD female mice starting at 2 weeks of age (Fig. 1a,b). As early as 2 weeks of age, various innate immune cells such as neutrophils (Ly6G<sup>+</sup>CD11b<sup>+</sup>) and pDCs (m927<sup>+</sup>CD11c<sup>med</sup>) and also B cells (CD19<sup>+</sup>) infiltrated the islets. The presence of neutrophils and pDCs was only transient, reaching a maximum at 3 and 4 weeks of age, respectively. Notably, the recruitment of these innate cells was specific to the NOD mice, as we did not observe such cells in the islets of C57BL/6 or BALB/c mice (Supplementary Fig. 1a,b).

Histological analysis confirmed the presence of pDCs (B220<sup>+</sup>CD11c<sup>+</sup>), conventional DCs (cDCs) (B220<sup>-</sup>CD11c<sup>+</sup>), B cells (B220<sup>+</sup>CD11c<sup>-</sup>) and neutrophils (NIMP-R14<sup>+</sup>) surrounding or inside the NOD islets at 3 but not at 6 weeks of age (Fig. 1c,d and Supplementary Fig. 2). Together, these data reveal that innate cells infiltrate the pancreatic islets of young NOD mice, which suggests they have a role in T1D initiation.

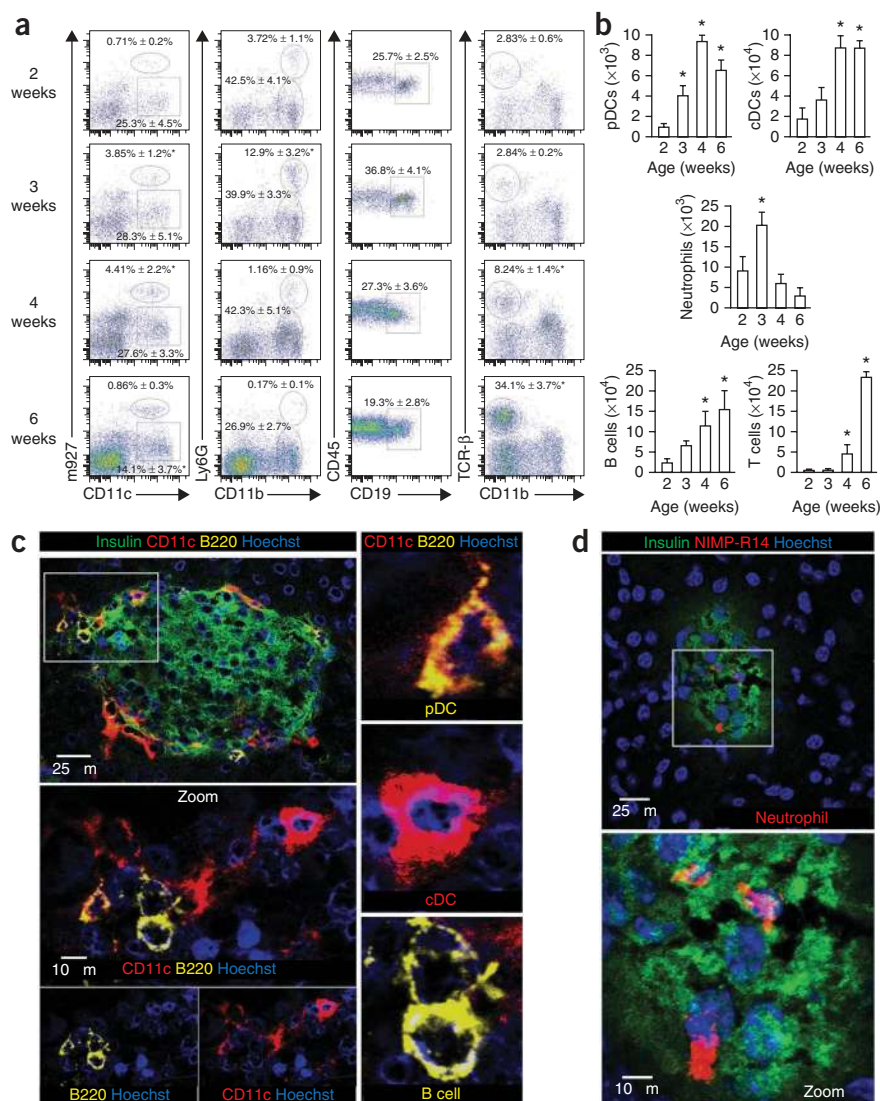
### Pancreatic IFN- $\alpha$ -secreting pDCs are crucial for T1D initiation

We analyzed IFN- $\alpha$  production in the islets of NOD mice because this cytokine is associated with activated pDCs and autoimmunity<sup>3</sup>. IFN- $\alpha$  was detected in the islets only at 3 weeks of age (Fig. 2a). To determine the association of IFN- $\alpha$  with T1D development, we analyzed the mRNA expression of IFN- $\alpha$ , IFN- $\alpha$ -induced gene products (ISG15, IRF7, IFIT1 and IFIT3) and proinflammatory gene products

<sup>1</sup>Institut National de la Santé et de la Recherche Médicale (INSERM), U986, Paris, France. <sup>2</sup>Université Paris Descartes Sorbonne Paris Cité, Laboratoire d'Excellence Inflamex, Paris, France. <sup>3</sup>INSERM, U781, Necker Hospital, Paris, France. <sup>4</sup>Department of Medical Biochemistry and Biophysics, Karolinska Institute, Stockholm, Sweden. <sup>5</sup>Dynavax Technologies Corporation, Berkeley, California, USA. <sup>6</sup>These authors contributed equally to this work. Correspondence should be addressed to A.L. or J.D. (agnes.lehuen@inserm.fr or julien.diana@inserm.fr).

Received 23 July; accepted 19 November; published online 16 December 2012; doi:10.1038/nm.3042

**Figure 1** Innate immune cells infiltrate the pancreas of NOD mice in the first postnatal weeks. **(a,b)** FACS analysis of CD45<sup>+</sup> infiltrating cells from pancreatic islets collected from 2 to 6 weeks. Frequencies of pDCs (m927<sup>+</sup>CD11c<sup>+</sup>), cDCs (m927<sup>-</sup>CD11c<sup>+</sup>), neutrophils (Ly6G<sup>+</sup>CD11b<sup>+</sup>), B cells (CD19<sup>+</sup>) and T cells (TCR $\beta$ <sup>+</sup>) are shown in each quadrant. Frequencies of positive cells among CD45<sup>+</sup> cells are represented in **a** and absolute number in **b**. Data are mean values  $\pm$  s.e.m. and are representative of four independent experiments with four pooled mice for each group. \* $P < 0.05$  for each group compared to 2-week-old group. **(c,d)** Immunohistological analysis of DCs **(c)** and neutrophils **(d)** from the pancreas of 3-week-old NOD mice. Zoomed-in boxed area in **c** shows cDCs (CD11c<sup>+</sup>) in red, B cells (B220<sup>+</sup>) in yellow and pDCs (CD11c<sup>+</sup>B220<sup>+</sup>) in orange and in **d** shows neutrophils (NIMPR14<sup>+</sup>) in red. Pancreatic sections were prepared as described in the Online Methods. Representative data from nine pancreases with ten sections for each pancreas from three independent experiments are shown. TCR- $\beta$ , T cell receptor- $\beta$ .



(interleukin-1 $\beta$ , IFN- $\gamma$  and CXCL10) in the islets of NOD mice at various ages. Expression of IFN- $\alpha$  and IFN- $\alpha$ -induced gene products reached a maximum at 3 and 4 weeks of age, respectively (**Supplementary Fig. 3**). Proinflammatory gene expression increased continually between 4 and 8 weeks of age in the islets of NOD mice (**Supplementary Fig. 3**). mRNA expression of IFN- $\alpha$  and IFN- $\alpha$ -induced gene products was not observed in nonautoimmune C57BL/6 or BALB/c mice (**Supplementary Figs. 3 and 4**). Together, these data reveal that the IFN- $\alpha$  signature in young mice was associated with the autoimmune-prone NOD genetic background. We next focused on pDCs and their putative role in T1D initiation. FACS analysis showed that pDCs isolated from the islets of NOD mice produced IFN- $\alpha$ , which peaked at 3 and declined at 6 weeks of age (**Fig. 2b**). Accordingly, the expression of IFN- $\alpha$ -induced genes in 4-week-old NOD mice was abolished after pDC depletion using m927 monoclonal antibody (mAb) against the BST2 antigen between 2 and 3 weeks of age (**Fig. 2c** and **Supplementary Fig. 5**). To assess the diabetogenic role of pDCs, we evaluated the autoreactive CD8<sup>+</sup> T cell response against the beta cell antigen islet-specific glucose-6-phosphatase catalytic subunit-related protein (IGRP)<sub>206-214</sub> in 8-week-old NOD mice that were depleted of pDCs or that had been treated with Siglec-H-specific mAb to prevent IFN- $\alpha$  production by pDCs (**Supplementary Fig. 6**). Both treatments administered between 2 and 3 weeks of age led to a dramatic reduction in the frequency of NRP-V7-tetramer<sup>+</sup> CD8<sup>+</sup> T cells specific for IGRP<sub>206-214</sub> within the pancreatic lymph nodes (PLN) and to a strong decrease in IGRP<sub>206-214</sub>-reactive IFN- $\gamma$ <sup>+</sup> CD8<sup>+</sup> T cells within the islets of 8-week-old NOD mice (**Fig. 2d** and **Supplementary Fig. 7**). Accordingly, pDC depletion in 2-week-old NOD mice prevented the development of T1D up to 30 weeks of age (**Fig. 2e**). Together, these data demonstrate that pancreatic pDCs produce IFN- $\alpha$  in young NOD mice and subsequently induce autoimmune diabetes. To determine whether Toll-like receptor (TLR)

pathways were necessary for IFN- $\alpha$  expression in the islets of NOD mice, we used *Myd88*<sup>-/-</sup> NOD mice, which lack the ability to signal through TLRs (excluding TLR3). We failed to detect IFN- $\alpha$  production in the islets from 3-week-old *Myd88*<sup>-/-</sup> NOD mice (**Supplementary Fig. 8a**). Accordingly, the increase in IFN- $\alpha$ -induced gene expression observed in NOD mice was also absent in the islets of 4-week-old *Myd88*<sup>-/-</sup> NOD mice (**Supplementary Fig. 8b**). To determine the TLR involved, we treated 2-week-old NOD mice with IRS<sub>954</sub>, an antagonist of TLR7 and TLR9 pathways. Such treatment decreased the expression of IFN- $\alpha$ -induced genes in the islets of 4-week-old NOD mice (**Supplementary Fig. 8b**). Finally, treatment of 2-week-old NOD mice with IRS<sub>954</sub> prevented the development of T1D, whereas CpG<sub>1585</sub>, a TLR9 agonist, increased the incidence of T1D, confirming the role of TLR7 and TLR9 and subsequent IFN- $\alpha$  production in the initiation of T1D in young NOD mice (**Fig. 2e**).

### B-1a cells activate pDCs in the pancreas

During psoriasis and lupus development, self DNA released from dying keratinocytes forms immune complexes with IgGs specific for double-stranded DNA (dsDNA), which then activate pDCs via TLR9 (ref. 4). Thus, we investigated whether this mechanism of pDC activation takes place in T1D. First, we detected dsDNA-specific IgGs

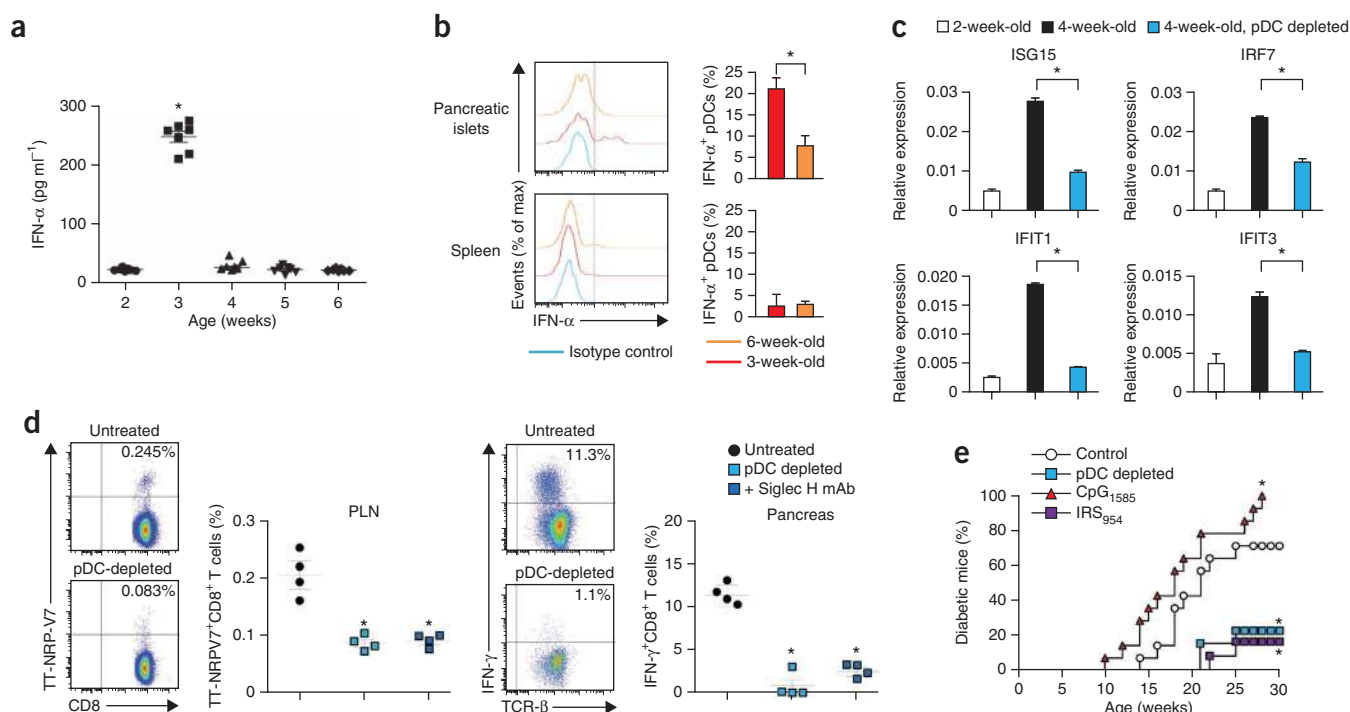


**Figure 2** Pancreatic pDCs express IFN- $\alpha$  and are required for T1D development in NOD mice. **(a)** IFN- $\alpha$  production in the islets of NOD mice from 2 to 6 weeks of age, measured after 36-h culture. Data represent seven independent mice for each group from four independent experiments. \* $P < 0.05$  for each group compared to 2-week-old group. **(b)** FACS analysis of IFN- $\alpha$  by pDCs from islets of 3- or 6-week-old NOD mice. Frequency (left) and absolute number (right) of IFN- $\alpha$ <sup>+</sup> cells among pDCs in pancreatic islets (top) and the spleen (bottom). Data are mean values  $\pm$  s.e.m. of four independent experiments with four pooled mice for each group. \* $P < 0.05$  for 3-week-old group compared to 6-week-old group. **(c)** mRNA expression of IFN- $\alpha$ -induced genes as assessed by quantitative PCR in the islets of NOD mice treated with depleting m927 mAb or isotype control. Data are mean values  $\pm$  s.e.m. of three independent experiments with four independent mice for each group. \* $P < 0.05$ . **(d)** Analysis of CD8<sup>+</sup> T cells specific for IGRP<sub>206–214</sub> in 8-week-old NOD mice after pDC depletion or blockade of IFN- $\alpha$ -producing-pDCs at 2–3 weeks of age. Left, frequency of NRPV7 tetramer-specific cells among the CD8<sup>+</sup> T cell population from PLN. Right, frequency of IFN- $\gamma$ <sup>+</sup> cells among the CD8<sup>+</sup> T cell population after re-stimulation with IGRP<sub>206–214</sub> peptide. Representative dot plots are shown, and values in the graph correspond to four independent mice for each group from two independent experiments. \* $P < 0.05$  for treated group compared untreated group. **(e)** Incidence of diabetes in NOD mice after pDC depletion or TLR9 targeting. Mice were treated with m927 mAb, isotype control, IRS<sub>954</sub> or CpG<sub>1585</sub> at 2 weeks of age over 2 weeks. \* $P < 0.05$  for each treated group compared to control group ( $n = 12$  mice per group).

at a low concentration in the sera of NOD, BALB/c and C57BL/6 mice and at a high concentration in serum from NZB/W F1 lupus-prone mice used as a positive control (Fig. 3a). Conversely, in the islets, we observed a higher amount of dsDNA-specific IgGs from NOD mice as compared to BALB/c or C57BL/6 mice (Fig. 3b). We also observed a higher amount of total IgG in islets from NOD mice compared to BALB/c or C57BL/6 mice (Supplementary Fig. 9). Among B cell populations, the CD5<sup>+</sup>CD19<sup>+</sup>CD1d<sup>med</sup> B-1a cells may produce high titers of dsDNA-specific IgGs<sup>18</sup>. Accordingly, we observed a large population of B-1a cells in the islets of NOD mice as early as 2 weeks of age (Fig. 3c). Their frequency among the total B cell population in the islets declined with the age (Fig. 3d and Supplementary Fig. 10).

Next, we performed peritoneal lavages between 1 to 3 weeks of age to deplete B-1a cells from pancreatic islets of NOD mice as previously described<sup>19</sup> (Supplementary Fig. 11). B-1a cell depletion largely reduced the production of dsDNA-specific IgGs in the islets of 3-week-old NOD mice (Fig. 3b). Additionally, pancreatic B-1a cells sorted from 3-week-old NOD mice produced dsDNA-specific IgGs after 7 d of culture, contrary to pancreatic B-2 cells (Fig. 3e). B-1a cell depletion also strongly reduced the frequency of IFN- $\alpha$ -secreting pDCs in the islets of 4-week-old NOD mice (Fig. 3f) and inhibited the diabetogenic T cell response within the PLN and islets of 8-week-old

NOD mice (Fig. 3g). Accordingly, B-1a cell depletion in 2-week-old NOD mice prevented T1D development (Fig. 3h). Collectively, these data unveil a crucial role of pancreatic B-1a cells in the activation of pDCs and T1D initiation.

### Pancreatic neutrophils activate pDCs and initiate T1D

Our analysis of the pancreatic infiltrate of 3-week-old NOD mice revealed the presence of neutrophils (Fig. 1). This group of innate cells is a key player in the clearance of extracellular pathogens<sup>20</sup>. In individuals with SLE, neutrophils secrete DNA-binding antimicrobial peptides (LL-37 in humans and CRAMP in mice) that bind immune complexes and potentiate their stimulatory effect on IFN- $\alpha$ -secreting pDCs<sup>21,22</sup>. We first observed that neutrophil depletion between 2 and 3 weeks of age using the NIMP-R14 mAb against Ly6G antigen (Supplementary Fig. 12) attenuated the expression of IFN- $\alpha$ -induced genes in the pancreas of 4-week-old NOD mice (Fig. 4a). Injection of CRAMP in 4-week-old NOD mice increased the expression of IFN- $\alpha$ -induced genes in the islets 24 h later (Fig. 4a). Moreover, coinciding with the presence of neutrophils, peak CRAMP mRNA expression was detected at 3 weeks of age (Fig. 4b), and neutrophil depletion markedly reduced this expression (Fig. 4c). FACS analysis confirmed that pancreatic neutrophils were the source of CRAMP in young NOD mice (Fig. 4d). No CRAMP expression was

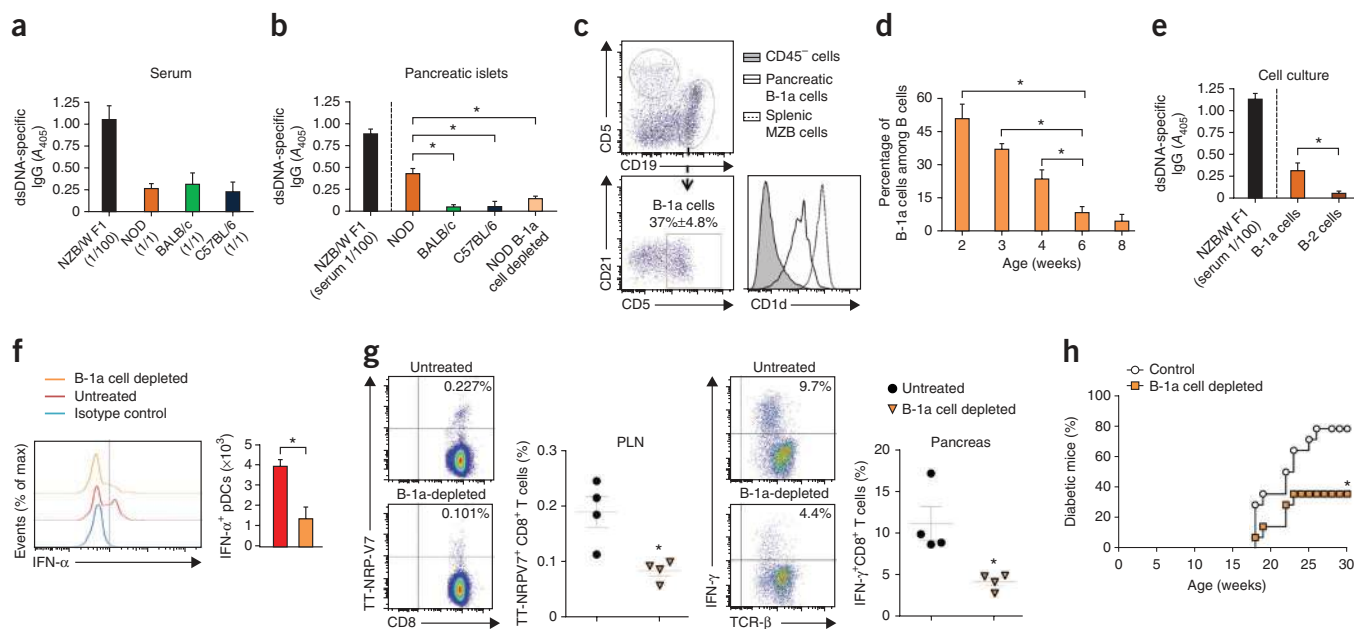


**Figure 3** B-1a cells activate pDCs in the pancreas and participate in the initiation of T1D. **(a,b)** dsDNA-specific IgG production in the serum **(a)** or in the islet supernatants **(b)** from 3-month-old NZB/W F1 mice or NOD, C57BL/6 and BALB/c mice at 3 weeks of age. In some conditions, B-1a cells were depleted in NOD mice as described in the Online Methods. Values are obtained by ELISA and are expressed as mean absorbance values at 405 nm with corrected cutoff values. Data are mean values  $\pm$  s.e.m. of two independent experiments with three independent mice for each group.  $*P < 0.05$ . **(c)** FACS analysis of B cell populations in the islets of NOD mice at 3 weeks of age. Frequency of B-1a cells (CD19<sup>+</sup>CD5<sup>+</sup>CD21<sup>-</sup>) among CD45<sup>+</sup> cells are represented, and representative expression of CD1d among CD45<sup>+</sup>CD19<sup>+</sup> cells is shown. **(d)** FACS analysis of B-1a cells in the islets of NOD mice at various ages. Frequencies of B-1a cells among CD45<sup>+</sup>CD19<sup>+</sup> cells are represented. Data are mean values  $\pm$  s.e.m. of four independent experiments with four pooled mice for each group.  $*P < 0.05$ . **(e)** dsDNA-specific IgG production in B-1a and B-2 cell cultures from 3-week-old NOD. Data are mean values  $\pm$  s.e.m. of two independent experiments with three independent mice for each group.  $*P < 0.05$ . **(f)** FACS analysis of IFN- $\alpha$  secretion by pDCs after B-1a cell depletion in NOD mice at 3 weeks of age. Right, absolute number of IFN- $\alpha$ <sup>+</sup> cells among pDCs. Data are mean values  $\pm$  s.e.m. of four independent experiments with four pooled mice for each group.  $*P < 0.05$ , treated group compared to untreated group. **(g)** Analysis of CD8<sup>+</sup> T cells specific for IGRP<sub>206–214</sub> in 8-week-old NOD mice after B-1a cell depletion at 2–3 weeks of age. Left, frequency of NRP-V7 tetramer-specific cells among CD8<sup>+</sup> T cell population from PLN. Right, frequency of IFN- $\gamma$ <sup>+</sup> cells among CD8<sup>+</sup> T cell population after re-stimulation with IGRP<sub>206–214</sub> peptide. Representative dot plots are shown, and values in the graphs correspond to four independent mice for each group from two independent experiments.  $*P < 0.05$  for treated group compared untreated group. **(h)** Incidence of diabetes in NOD mice after B-1a cell depletion in NOD mice. Mice were treated between 7 d and 21 d of age.  $*P < 0.05$  for treated group compared to control group ( $n = 12$  mice per group).

observed in other CD45<sup>+</sup> or in CD45<sup>-</sup> cells in the pancreatic islets (**Supplementary Fig. 13**). Histological analysis confirmed the presence of CRAMP-secreting neutrophils inside the islets of 3-week-old NOD mice (**Fig. 4e**). Pancreatic neutrophils appeared to release neutrophil extracellular traps (NETs), which are typically associated with CRAMP release and activation of IFN- $\alpha$ -secreting pDCs in patients with SLE<sup>21,22</sup>.

We confirmed that *ex vivo*-isolated pancreatic neutrophils produced NETs containing DNA by staining with a Ly6G-specific antibody and SYTOX-Green, and these NETs were associated with CRAMP peptide (**Fig. 4f** and **Supplementary Fig. 14**). Neutrophil depletion at 2 weeks of age reduced the frequency of IFN- $\alpha$ -secreting pDCs in the islets of treated NOD mice (**Fig. 5a**) and dampened the diabetogenic T cell response within the PLN and islets of 8-week-old NOD mice (**Fig. 5b**). Accordingly, neutrophil depletion in 2-week-old NOD mice inhibited T1D development at later ages (**Fig. 5c**). Together, these data support a role for CRAMP-secreting neutrophils in the activation of pancreatic pDCs and T1D initiation.

### Neutrophils and B-1a cells cooperate to activate pDCs

We next investigated the molecular interplay between innate cells in the islets of young NOD mice. Neutrophils are activated via various pathways including Fc $\gamma$  receptors (Fc $\gamma$ Rs), TLRs or both.

First, we excluded the TLR pathway because CRAMP mRNA expression in the islets was unaltered in *Myd88*<sup>-/-</sup> NOD mice as compared to WT NOD mice (**Fig. 4c**). As IgG-secreting B-1a cells have been shown to activate neutrophils via Fc $\gamma$ R20, we performed *in vitro* cultures with neutrophils isolated from bone marrow and activated with phorbol-12-myristate-13-acetate (PMA), immune complexes (dsDNA plus commercial dsDNA-specific IgGs) or B-1a immune complexes (dsDNA plus pancreatic B-1a cell-conditioned medium), and measured CRAMP expression on the surface of neutrophils (**Fig. 5d**). As expected, PMA (used as positive control) induced expression of CRAMP. Immune complexes and B-1a immune complexes also induced CRAMP expression, which was blocked by the addition of a mix of Fc $\gamma$ RII/III-specific and Fc $\gamma$ RIV-specific mAbs, revealing that the neutrophils were activated through Fc $\gamma$ Rs (**Fig. 5d**). Notably, our data obtained with severe combined immunodeficiency NOD mice, which are devoid of T and B cells, demonstrated the requirement of B cells in the activation of pancreatic neutrophils (**Supplementary Fig. 15**). These data strongly suggest that in the pancreatic islets of NOD mice, CRAMP-producing neutrophils are activated by IgG-secreting B-1a cells via Fc $\gamma$ Rs.

To determine whether both neutrophils and B-1a cells are required for activation of pDCs, we cultured splenic pDCs with pancreatic B-1a cell-conditioned medium, supernatant of bone marrow-isolated

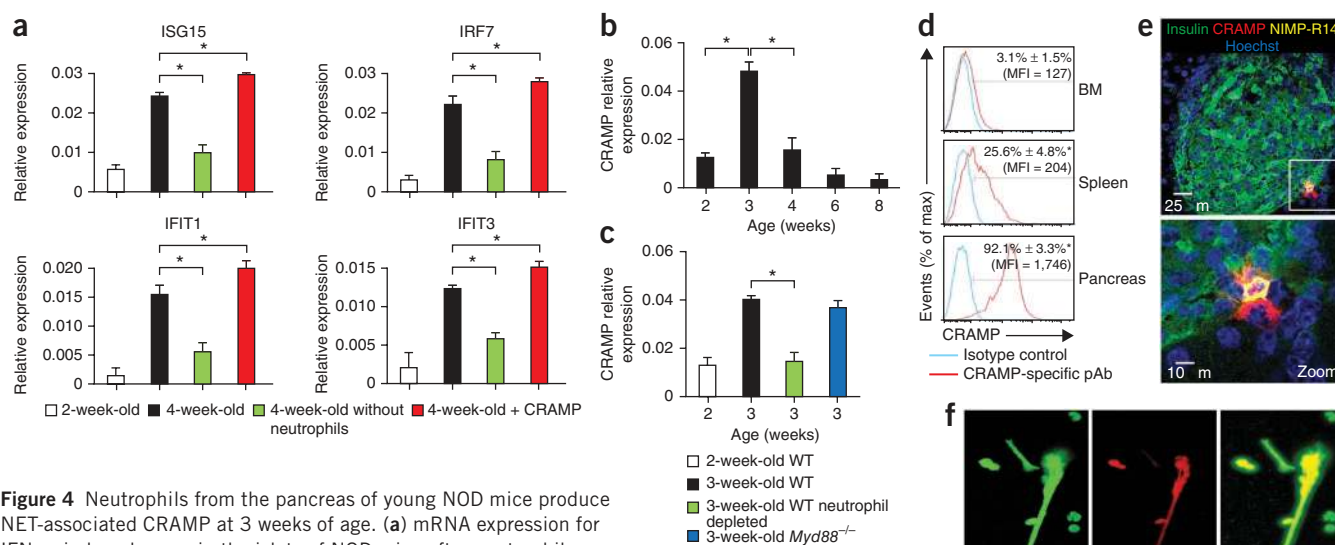


**Figure 4** Neutrophils from the pancreas of young NOD mice produce NET-associated CRAMP at 3 weeks of age. **(a)** mRNA expression for IFN- $\alpha$ -induced genes in the islets of NOD mice after neutrophil depletion or CRAMP peptide injection. Data are mean values  $\pm$  s.e.m. of two independent experiments with four independent mice for each group.  $*P < 0.05$ . **(b)** mRNA expression for CRAMP was analyzed in the islets of NOD mice at various ages. **(c)** CRAMP mRNA expression in the islets of WT NOD mice depleted or not depleted of neutrophils or in the islets of *Myd88*<sup>-/-</sup> NOD mice. Data are mean values  $\pm$  s.e.m. of two independent experiments with four independent mice for each group.  $*P < 0.05$ . **(d)** FACS analysis of CRAMP surface expression by neutrophils of NOD mice at 3 weeks of age. Data are the frequency of CRAMP<sup>+</sup> cells and mean fluorescence intensity (MFI) of CRAMP expression CD45<sup>+</sup> CD11b<sup>+</sup> Ly6G<sup>+</sup> cells. Data are mean values  $\pm$  s.e.m. of four independent experiments with four pooled mice for each group.  $*P < 0.05$  for each group compared to bone marrow (BM) group. **(e)** Immunohistological analysis of pancreatic neutrophils in 3-week-old NOD mice. Zoomed-in boxed area shows NETs released by the neutrophil. Representative data from six pancreases with ten sections for each pancreas from three independent experiments are shown. **(f)** The ability of neutrophils to form CRAMP-associated NETs *ex vivo* when isolated from islets of NOD at 3 weeks of age was determined by immunostaining. Representative data from five fields of cells from the islets of eight pooled mice from three independent experiments are shown.

neutrophils preactivated with B-1a immune complexes, or both. As a positive control of pDC activation, CpG<sub>1585</sub> induced IFN- $\alpha$  production in pDCs, which was inhibited by IRS<sub>954</sub> (Fig. 5e). Soluble IC induced moderate production of IFN- $\alpha$ , which was potentiated by the addition of CRAMP as previously described<sup>21</sup>. B-1a cell-conditioned medium also induced moderate IFN- $\alpha$  production that was potentiated by the addition of neutrophil-conditioned medium (Fig. 5e). This strong IFN- $\alpha$  production induced by the addition of both supernatants was inhibited by IRS954 (Fig. 5e). These data demonstrate that B-1a cells secreting dsDNA-specific IgG and CRAMP-secreting neutrophils cooperate to stimulate IFN- $\alpha$  production by pDCs through TLR9.

### Beta cell death initiates the innate cell activation cascade

Our data revealed that an innate cell crosstalk takes place in the pancreas of young NOD mice and leads to the initiation of T1D. However, the initial event that triggers this crosstalk remained unclear. We investigated the putative role of physiological beta cell death that occurs spontaneously in young NOD mice during organogenesis and after weaning<sup>13</sup>. To mimic this event, we induced beta cell death by injecting streptozotocin (STZ). On day 1 after STZ injection in 6-week-old NOD mice, we observed an increase in the expression of IFN- $\alpha$ -induced genes in the islets (Fig. 6a). This increase was dependent on pDCs, as revealed by m927 depleting mAb treatment (Fig. 6b). STZ treatment failed to induce expression of IFN- $\alpha$ -induced genes and recruitment of pDCs, neutrophils or B-1a cells in the islets of non-autoimmune-prone C57BL/6 and BALB/c mice (Supplementary Figs. 16 and 17a).

We next demonstrated that STZ treatment at 6 weeks of age induced the production of dsDNA-specific IgGs and increased the frequency of CRAMP-expressing neutrophils in the islets of NOD mice 24 h later (Fig. 6c,d and Supplementary Fig. 17b). This increased production of dsDNA-specific IgGs and the recruitment of CRAMP<sup>+</sup> neutrophils in the islets induced by STZ were similar to that which we observed in 3-week-old NOD mice, suggesting that beta cell death could be required for the activation of pancreatic pDCs in young NOD mice. To test this hypothesis, we treated 7-d-old NOD mice with a single injection of Z-VAD, a pan-caspase inhibitor. This treatment abrogated dsDNA-specific IgG secretion, CRAMP-production by neutrophils and IFN- $\alpha$ -induced gene expression in islets of 4-week-old NOD mice (Fig. 6e-g) and prevented T1D development up to 30 weeks of age (Fig. 6h). Altogether, our study demonstrated that in young NOD mice, physiological beta cell death initiates the activation of innate immune cells, which leads to the local production of IFN- $\alpha$ , the development of diabetogenic T cell responses and autoimmune diabetes.

### DISCUSSION

Despite increased knowledge of the pathogenesis of T1D, the early stages of disease pathogenesis remain poorly defined. Here, we demonstrate that in young NOD mice, when physiological beta cell death occurs, innate immune cell crosstalk takes place in the pancreas that is crucial for T1D development (Supplementary Fig. 18). We propose that beta cell debris (that is, self DNA) form immune complexes with dsDNA-specific IgGs secreted by B-1a cells. Neutrophils produce DNA-binding peptide that potentiates these immune complexes, inducing IFN- $\alpha$  secretion by pancreatic pDCs through TLR9.

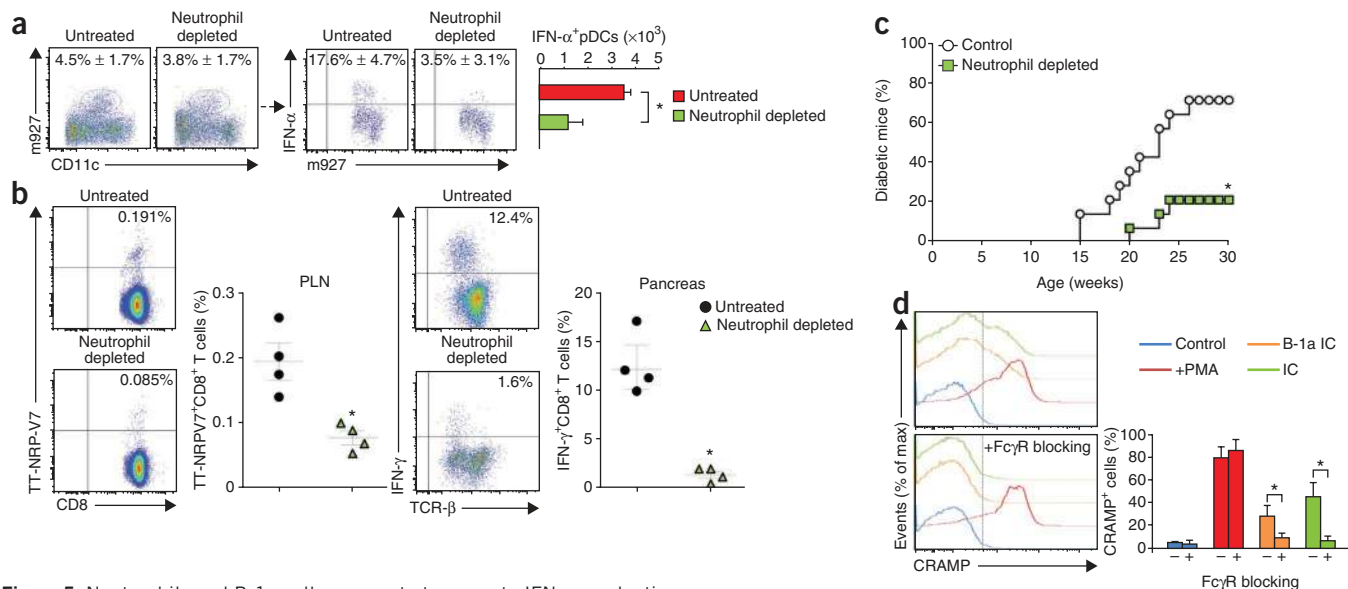


**Figure 5** Neutrophils and B-1a cells cooperate to promote IFN- $\alpha$  production by pDCs. **(a)** FACS analysis of IFN- $\alpha$  secretion by pDCs after neutrophil depletion in NOD mice at 3 weeks of age. Frequency of pDCs (left), frequency (middle) and absolute number of IFN- $\alpha$ <sup>+</sup> cells among pDCs (right) are represented. Data are mean values  $\pm$  s.e.m. of four independent experiments with four pooled mice for each group. \* $P$  < 0.05, treated group compared to untreated group. **(b)** Analysis of CD8<sup>+</sup> T cells specific for IGRP<sub>206-214</sub> in 8-week-old NOD mice after neutrophil depletion at 2–3 weeks of age. Left, frequency of NRP-V7 tetramer-specific cells among CD8<sup>+</sup> T cell population from PLN. Right, frequency of IFN- $\gamma$ <sup>+</sup> cells among CD8<sup>+</sup> T cell population after restimulation with IGRP<sub>206-214</sub> peptide. Representative dot plots are shown, and values in the graphs correspond to four independent mice for each group from two independent experiments. \* $P$  < 0.05 for treated group compared to untreated group. **(c)** Incidence of diabetes in NOD mice after neutrophil depletion in NOD mice. Mice were treated with NIMP-R14 mAb or isotype control between 7 and 21 d of age. \* $P$  < 0.05 for treated group compared to control group ( $n$  = 12 mice per group). **(d)** FACS analysis of surface expression of CRAMP by neutrophils after *in vitro* culture. Bone marrow neutrophils were added to PMA, immobilized immune complexes (IC) or B-1a IC and cultured for 20 min. In some conditions, neutrophils were preincubated with Fc $\gamma$ R-blocking mAbs. Data are mean values  $\pm$  s.e.m. of four independent experiments. \* $P$  < 0.05, each group compared to control group. **(e)** IFN- $\alpha$  production evaluated by ELISA in *in vitro* pDC culture in the presence of neutrophil or B-1a cell-conditioned medium. pDCs were isolated from the spleen of 3-week-old NOD mice and were incubated with CpG<sub>1585</sub>, soluble IC or CRAMP (left) or cultured with neutrophil-conditioned medium and/or B-1a cell-conditioned medium (right), all in the presence or absence of TLR7 and TLR9 inhibitor (IRS<sub>954</sub>). Data are mean values  $\pm$  s.e.m. of three independent experiments with four pooled mice for each group. \* $P$  < 0.05.

This cytokine creates an inflammatory milieu favorable for the diabetogenic adaptive response and autoimmune diabetes.

Aside from the key role of IFN- $\alpha$ -secreting pDCs in antiviral defense, a growing body of evidence argues for a pathogenic role for them in several autoimmune diseases such as psoriasis and lupus<sup>23</sup>. In T1D, differing results are found in the literature concerning the role of IFN- $\alpha$  and pDCs in disease pathogenesis. The expansion of IFN- $\alpha$ -producing pDCs has been documented in patients with T1D around the time of diagnosis<sup>8</sup>, and IFN- $\alpha$  treatment of patients with hepatitis infection or with leukemia has been shown to induce diabetes development<sup>6,7,24</sup>. Recent studies revealed that NOD mice harbor high IFN- $\alpha$  levels in PLN before the onset of diabetes<sup>25</sup> and that pDC depletion prevents T1D development in these mice<sup>26</sup>. NOD mice harbor substantially more splenic pDCs in comparison to C57BL/6 mice, and NOD pDCs produce more IFN- $\alpha$  after *in vitro* stimulation than C57BL/6 pDCs<sup>27</sup>. Paradoxically, older studies showed that IFN- $\alpha$  treatment reduces diabetes incidence in NOD mice or Biobreeding (BB) rats, a strain of rats that spontaneously develop autoimmune diabetes<sup>28-31</sup>. However, treatment with an inducer of IFN- $\alpha$  and IFN- $\beta$  production such as poly(I:C) can prevent<sup>32,33</sup> or accelerate<sup>34-36</sup>

the disease depending on the dose, time, duration and route of administration (oral, intraperitoneal or subcutaneous). The pro-inflammatory role of type I IFNs has been extensively documented; IFN- $\alpha$  and IFN- $\beta$  induce cDC maturation, activate immunoglobulin-secreting B cells, enhance CRAMP expression by neutrophils and boost effector T cell responses<sup>37,38</sup>. Type I IFNs also directly affect pancreatic beta cells by inducing cytokine and chemokine secretion and major histocompatibility complex class I expression, enhancing their susceptibility to attack from diabetogenic T cells<sup>39</sup>. The protective role of IFN- $\alpha$  treatment remains unclear; one hypothesis is that type I IFN can boost the activity of regulatory T cells<sup>40-43</sup>.

It has been also reported in some diabetes models that pDCs can exert disease-protective effects against the development of T1D<sup>44,45</sup>. However, the precise mechanism leading to T1D prevention and the direct role of pDCs were not precisely addressed. In our previous studies<sup>46,47</sup>, we demonstrated that during viral infection of 6-week-old NOD mice, pDCs can inhibit T1D development by two complementary pathways but at different times and locations. Indeed, 1–2 d after infection, pDCs transiently produced IFN- $\alpha$  in the pancreas to dampen viral replication, avoiding tissue damage, and then migrate to the PLN

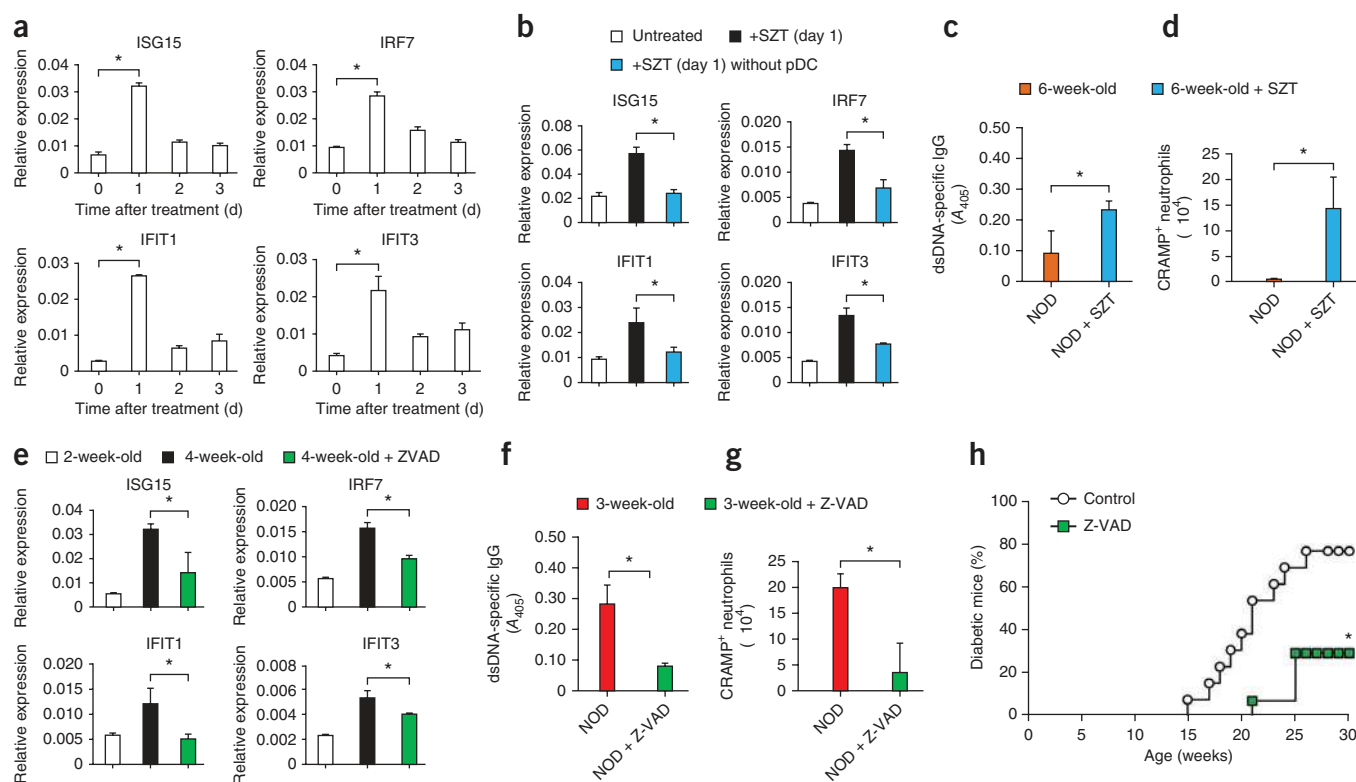


**Figure 6** Initial beta cell death is required to induce innate cell activation and T1D development. **(a,b)** mRNA expression for IFN- $\alpha$ -induced genes in islets from 6-week-old NOD mice after injection of STZ. In some conditions **(b)**, pDCs were depleted 1 d before the injection of STZ. Data are mean values  $\pm$  s.e.m. of two independent experiments with four independent mice for each group.  $*P < 0.05$ . **(c)** DNA-specific IgG production in the islet supernatants from 6-week-old NOD mice 12 h after STZ injection. Data are mean values  $\pm$  s.e.m. of two independent experiments with two independent mice for each group.  $*P < 0.05$ . **(d)** FACS analysis of CRAMP expression by pancreatic neutrophils from 6-week-old NOD mice 12 h after STZ injection. Absolute number of CRAMP<sup>+</sup> cells among CD45<sup>+</sup>CD11b<sup>+</sup>Ly6G<sup>+</sup> cells is represented. Data are mean values  $\pm$  s.e.m. of four independent experiments with two pooled mice for each group.  $*P < 0.05$ . **(e)** mRNA expression for IFN- $\alpha$ -induced genes in islets of 2- or 4-week-old NOD mice after Z-VAD treatment. Data are mean values  $\pm$  s.e.m. of two independent experiments with four independent mice for each group.  $*P < 0.05$ . **(f)** DNA-specific IgG production in the islet supernatants from 3-week-old NOD mice treated or not with Z-VAD. Data are mean values  $\pm$  s.e.m. of two independent experiments with two independent mice for each group.  $*P < 0.05$ . **(g)** FACS analysis of CRAMP expression by pancreatic neutrophils from 3-week-old NOD mice treated or not with Z-VAD. Absolute number of CRAMP<sup>+</sup> cells among CD45<sup>+</sup>CD11b<sup>+</sup>Ly6G<sup>+</sup> cells is represented. Data are mean values  $\pm$  s.e.m. of four independent experiments with two pooled mice for each group.  $*P < 0.05$ . **(h)** Incidence of diabetes in NOD mice after blockade of apoptosis by Z-VAD treatment. Mice were treated with Z-VAD at 7 d of age.  $*P < 0.05$  for treated group compared to control group ( $n = 12$  mice per group).

and produce transforming growth factor- $\beta$ , which induces regulatory T cells at later time points. However, to be efficient, these mechanisms of protection required the stimulation of invariant natural killer T cells at the time of infection. Altogether, these studies support the notion that pDCs could harbor both pathogenic and protective functions during autoimmune diabetes development, depending on the course of the disease, the infectious context and the localization of the cells.

B cells are proposed to be involved in T1D pathogenesis as self antigen-presenting cells, but there is little evidence for a diabetogenic role for autoantibodies<sup>48</sup>. Our data revealed that the innate-like CD5<sup>+</sup> B-1a cells have an as yet undescribed role in T1D initiation through the production of dsDNA-specific IgGs and the activation of neutrophils and pDCs in the pancreas. A previous publication showed that peritoneal B-1a cells participate in T1D development in NOD mice, but their mechanism of action remained unknown<sup>19</sup>. Notably, the number of circulating CD5<sup>+</sup> B cells is higher in children with a very recent onset of T1D, as compared with patients with long-term disease or controls<sup>49</sup>. An altered B cell receptor signaling threshold has also been observed in patients with T1D as compared to healthy controls<sup>50</sup>. High frequencies of CD5<sup>+</sup> B cells have been reported in patients with

other autoimmune diseases, such as Sjögren's disease<sup>51</sup> and rheumatoid arthritis<sup>52</sup>. Similarly, NOD mice harbor an elevated frequency of self-reactive B cells compared to C57BL/6 and BALB/c mice<sup>53</sup>.

The role of neutrophils in autoimmunity has been described in small-vessel vasculitis, SLE, psoriasis and a mouse model of skin inflammation<sup>21,22,54,55</sup>. In these studies, neutrophils act by producing the DNA-binding peptides LL-37 and CRAMP, which form complexes with self DNA and dsDNA-specific IgGs, activating IFN- $\alpha$  production by pDCs. DNA-binding peptides are released by neutrophils during NETosis<sup>20</sup>. Our study demonstrates that neutrophils release NET-associated CRAMP in pancreatic islets, which promotes diabetes initiation in NOD mice.

We show that spontaneous or STZ-induced beta cell death is required for the activation of IFN- $\alpha$ -secreting pDCs probably by releasing self DNA essential to the formation of immune complexes, as shown in other diseases<sup>56</sup>. Previous studies in NOD mice provided evidence that beta cell death naturally occurring during the first post-natal weeks initiates the activation of cDCs and the priming of auto-reactive T cells<sup>14</sup>. Notably, these waves of physiological beta cell death also occur in pigs<sup>15</sup> and humans<sup>16</sup>. Beta cell debris could accumulate

in the pancreas of NOD mice because of a defect in phagocytic clearance in this genetic background<sup>17</sup>. Previous data indicate that proinflammatory responses and autoimmune disorders can be elicited by defective clearance of apoptotic cells<sup>57</sup>. During infancy, the immune system may be provoked with a physiological massive rebuilding of the pancreatic islets via programmed cell death and may initiate the diabetogenic process in an autoimmune genetic background<sup>58</sup>.

Finally, the interplay between B-1a cells, neutrophils and pDCs seems to be a common feature of autoimmune diseases. This new aspect of the pathogenesis of autoimmune diseases is likely to open new therapeutic avenues directed toward the targeting of innate immune cells. One of the major needs is to set up more efficient tools that allow the detection of these primary diabetogenic events. Approaches focused on pDCs would be more selective and tolerable than targeting of the IFN- $\alpha$  response, which can disturb antiviral responses.

## METHODS

Methods and any associated references are available in the [online version of the paper](#).

*Note: Supplementary information is available in the online version of the paper.*

## ACKNOWLEDGMENTS

We thank N. Charles (INSERM UMR-S 699, Paris Diderot University) for dsDNA-specific immunoglobulin ELISA, M. Colonna (Department of Pathology and Immunology, Washington University School of Medicine) for m927 mAb, S. Mecheri (Biology of Host Parasite Interactions Unit, Pasteur Institute) for NIMP-14 mAb, S. Muller (CNRS, Institut de Biologie Moléculaire et Cellulaire, UPR9021) for serum from NZB/W F1 mice, J. Ravetch (Laboratory of Molecular Genetics and Immunology, Rockefeller University) for Fc $\gamma$ RIV-specific mAb, N. Thieblemont (CNRS UMR 8147, Paris Descartes University) for *Myd88*<sup>-/-</sup> NOD mice and all for their expertise. We thank F. Boutillon for technical assistance and the staff of the INSERM U986 mouse facility for help in animal care. Y.S. is supported by a doctoral fellowship from the Region Ile de France. This work was supported by funds from INSERM, Centre National de la Recherche Scientifique, ANR-05-PCOD009-01, ANR-09-GENO-023 and Labex INFLAMEX to A.L. A.L. is recipient of an APHP-CNRS Contrat Hospitalier de Recherche Translationnelle.

## AUTHOR CONTRIBUTIONS

J.D. initiated and led the whole project, coordinated with different investigators, designed and performed experiments, analyzed the data and wrote the manuscript; Y.S. designed and performed experiments, analyzed the data and wrote the manuscript; L.F. did confocal microscopy experiments, analyzed the data and wrote the manuscript; L.B. provided technical assistance; B.A. and F.B. provided intellectual input and key reagents for neutrophil and pDC analysis; and A.L. was responsible for project planning, data analysis, discussion and writing.

## COMPETING FINANCIAL INTERESTS

The authors declare no competing financial interests.

Published online at <http://www.nature.com/doi/10.1038/nm.3042>.

Reprints and permissions information is available online at <http://www.nature.com/reprints/index.html>.

- Coppieters, K.T. *et al.* Demonstration of islet-autoreactive CD8 T cells in insulinitic lesions from recent onset and long-term type 1 diabetes patients. *J. Exp. Med.* **209**, 51–60 (2012).
- Lehuen, A., Diana, J., Zaccane, P. & Cooke, A. Immune cell crosstalk in type 1 diabetes. *Nat. Rev. Immunol.* **10**, 501–513 (2010).
- Reizis, B., Bunin, A., Ghosh, H.S., Lewis, K.L. & Sisirak, V. Plasmacytoid dendritic cells: recent progress and open questions. *Annu. Rev. Immunol.* **29**, 163–183 (2011).
- Gilliet, M., Cao, W. & Liu, Y.J. Plasmacytoid dendritic cells: sensing nucleic acids in viral infection and autoimmune diseases. *Nat. Rev. Immunol.* **8**, 594–606 (2008).
- Swiecki, M. & Colonna, M. Unraveling the functions of plasmacytoid dendritic cells during viral infections, autoimmunity, and tolerance. *Immunol. Rev.* **234**, 142–162 (2010).
- Fabris, P. *et al.* Insulin-dependent diabetes mellitus during  $\alpha$ -interferon therapy for chronic viral hepatitis. *J. Hepatol.* **28**, 514–517 (1998).
- Guerci, A.P. *et al.* Onset of insulin-dependent diabetes mellitus after interferon- $\alpha$  therapy for hairy cell leukaemia. *Lancet* **343**, 1167–1168 (1994).
- Allen, J.S. *et al.* Plasmacytoid dendritic cells are proportionally expanded at diagnosis of type 1 diabetes and enhance islet autoantigen presentation to T-cells through immune complex capture. *Diabetes* **58**, 138–145 (2009).
- Winkler, C. *et al.* An interferon-induced helicase (IFIH1) gene polymorphism associates with different rates of progression from autoimmunity to type 1 diabetes. *Diabetes* **60**, 685–690 (2011).
- Stewart, T.A. *et al.* Induction of type 1 diabetes by interferon- $\alpha$  in transgenic mice. *Science* **260**, 1942–1946 (1993).
- Alba, A. *et al.* IFN- $\beta$  accelerates autoimmune type 1 diabetes in nonobese diabetic mice and breaks the tolerance to beta cells in nondiabetes-prone mice. *J. Immunol.* **173**, 6667–6675 (2004).
- Trudeau, J.D. *et al.* Neonatal beta-cell apoptosis: a trigger for autoimmune diabetes? *Diabetes* **49**, 1–7 (2000).
- Mathis, D., Vence, L. & Benoist, C. Beta-cell death during progression to diabetes. *Nature* **414**, 792–798 (2001).
- Turley, S., Poirot, L., Hattori, M., Benoist, C. & Mathis, D. Physiological beta cell death triggers priming of self-reactive T cells by dendritic cells in a type-1 diabetes model. *J. Exp. Med.* **198**, 1527–1537 (2003).
- Bock, T., Kyhnel, A., Pakkenberg, B. & Buschard, K. The postnatal growth of the beta-cell mass in pigs. *J. Endocrinol.* **179**, 245–252 (2003).
- Kassem, S.A., Ariel, I., Thornton, P.S., Scheimberg, I. & Glaser, B. Beta-cell proliferation and apoptosis in the developing normal human pancreas and in hyperinsulinism of infancy. *Diabetes* **49**, 1325–1333 (2000).
- O'Brien, B.A. *et al.* A deficiency in the *in vivo* clearance of apoptotic cells is a feature of the NOD mouse. *J. Autoimmun.* **26**, 104–115 (2006).
- Baumgarth, N. The double life of a B-1 cell: self-reactivity selects for protective effector functions. *Nat. Rev. Immunol.* **11**, 34–46 (2011).
- Kendall, P.L., Woodward, E.J., Hulbert, C. & Thomas, J.W. Peritoneal B cells govern the outcome of diabetes in non-obese diabetic mice. *Eur. J. Immunol.* **34**, 2387–2395 (2004).
- Mantovani, A., Cassatella, M.A., Costantini, C. & Jaillon, S. Neutrophils in the activation and regulation of innate and adaptive immunity. *Nat. Rev. Immunol.* **11**, 519–531 (2011).
- Lande, R. *et al.* Neutrophils activate plasmacytoid dendritic cells by releasing self-DNA-peptide complexes in systemic lupus erythematosus. *Sci. Transl. Med.* **3**, 73ra19 (2011).
- Garcia-Romo, G.S. *et al.* Netting neutrophils are major inducers of type 1 IFN production in pediatric systemic lupus erythematosus. *Sci. Transl. Med.* **3**, 73ra20 (2011).
- Lande, R. & Gilliet, M. Plasmacytoid dendritic cells: key players in the initiation and regulation of immune responses. *Ann. NY Acad. Sci.* **1183**, 89–103 (2010).
- Fabris, P. *et al.* Type 1 diabetes mellitus in patients with chronic hepatitis C before and after interferon therapy. *Aliment. Pharmacol. Ther.* **18**, 549–558 (2003).
- Li, Q. *et al.* Interferon- $\alpha$  initiates type 1 diabetes in nonobese diabetic mice. *Proc. Natl. Acad. Sci. USA* **105**, 12439–12444 (2008).
- Li, Q. & McDevitt, H.O. The role of interferon  $\alpha$  in initiation of type 1 diabetes in the NOD mouse. *Clin. Immunol.* **140**, 3–7 (2011).
- Peng, R.H., Paek, E., Xia, C.Q., Tennyson, N. & Clare-Salzler, M.J. Heightened interferon- $\alpha/\beta$  response causes myeloid cell dysfunction and promotes T1D pathogenesis in NOD mice. *Ann. NY Acad. Sci.* **1079**, 99–102 (2006).
- Sobel, D.O. & Ahvazi, B.  $\alpha$ -interferon inhibits the development of diabetes in NOD mice. *Diabetes* **47**, 1867–1872 (1998).
- Sobel, D.O. *et al.* Low dose poly I:C prevents diabetes in the diabetes prone BB rat. *J. Autoimmun.* **11**, 343–352 (1998).
- Brod, S.A., Malone, M., Darcan, S., Papolla, M. & Nelson, L. Ingested interferon  $\alpha$  suppresses type 1 diabetes in non-obese diabetic mice. *Diabetologia* **41**, 1227–1232 (1998).
- Tanaka-Kataoka, M. *et al.* Oral use of interferon- $\alpha$  delays the onset of insulin-dependent diabetes mellitus in nonobese diabetic mice. *J. Interferon Cytokine Res.* **19**, 877–879 (1999).
- Serreze, D.V., Hamaguchi, K. & Leiter, E.H. Immunostimulation circumvents diabetes in NOD/Lt mice. *J. Autoimmun.* **2**, 759–776 (1989).
- Zhou, R., Wei, H. & Tian, Z. NK3-like NK cells are involved in protective effect of polyinosinic-polycytidylic acid on type 1 diabetes in nonobese diabetic mice. *J. Immunol.* **178**, 2141–2147 (2007).
- Ewel, C.H., Sobel, D.O., Zeligs, B.J. & Bellanti, J.A. Poly I:C accelerates development of diabetes mellitus in diabetes-prone BB rat. *Diabetes* **41**, 1016–1021 (1992).
- Sobel, D.O. *et al.* Poly I:C induces development of diabetes mellitus in BB rat. *Diabetes* **41**, 515–520 (1992).
- Huang, X., Hultgren, B., Dybdal, N. & Stewart, T.A. Islet expression of interferon- $\alpha$  precedes diabetes in both the BB rat and streptozotocin-treated mice. *Immunity* **1**, 469–478 (1994).
- Theofilopoulos, A.N., Kono, D.H., Beutler, B. & Baccala, R. Intracellular nucleic acid sensors and autoimmunity. *J. Interferon Cytokine Res.* **31**, 867–886 (2011).
- Desmet, C.J. & Ishii, K.J. Nucleic acid sensing at the interface between innate and adaptive immunity in vaccination. *Nat. Rev. Immunol.* **12**, 479–491 (2012).
- Lang, K.S. *et al.* Toll-like receptor engagement converts T-cell autoreactivity into overt autoimmune disease. *Nat. Med.* **11**, 138–145 (2005).
- Aune, T.M. & Pierce, C.W. Activation of a suppressor T-cell pathway by interferon. *Proc. Natl. Acad. Sci. USA* **79**, 3808–3812 (1982).



41. Mujtaba, M.G., Soos, J.M. & Johnson, H.M. CD4 T suppressor cells mediate interferon  $\tau$  protection against experimental allergic encephalomyelitis. *J. Neuroimmunol.* **75**, 35–42 (1997).
42. Teige, I., Liu, Y. & Issazadeh-Navikas, S. IFN- $\beta$  inhibits T cell activation capacity of central nervous system APCs. *J. Immunol.* **177**, 3542–3553 (2006).
43. González-Navajas, J.M., Lee, J., David, M. & Raz, E. Immunomodulatory functions of type I interferons. *Nat. Rev. Immunol.* **12**, 125–135 (2012).
44. Kared, H. *et al.* Treatment with granulocyte colony-stimulating factor prevents diabetes in NOD mice by recruiting plasmacytoid dendritic cells and functional CD4<sup>+</sup>CD25<sup>+</sup> regulatory T-cells. *Diabetes* **54**, 78–84 (2005).
45. Saxena, V., Ondr, J.K., Magnusen, A.F., Munn, D.H. & Katz, J.D. The countervailing actions of myeloid and plasmacytoid dendritic cells control autoimmune diabetes in the nonobese diabetic mouse. *J. Immunol.* **179**, 5041–5053 (2007).
46. Diana, J. *et al.* Viral infection prevents diabetes by inducing regulatory T cells through NKT cell–plasmacytoid dendritic cell interplay. *J. Exp. Med.* **208**, 729–745 (2011).
47. Diana, J. *et al.* NKT cell–plasmacytoid dendritic cell cooperation via OX40 controls viral infection in a tissue-specific manner. *Immunity* **30**, 289–299 (2009).
48. Mallone, R. & Brezar, V. To B or not to B: (anti) bodies of evidence on the crime scene of type 1 diabetes? *Diabetes* **60**, 2020–2022 (2011).
49. De Filippo, G. *et al.* Increased CD5<sup>+</sup>CD19<sup>+</sup> B lymphocytes at the onset of type 1 diabetes in children. *Acta Diabetol.* **34**, 271–274 (1997).
50. Habib, T. *et al.* Altered B cell homeostasis is associated with type 1 diabetes and carriers of the PTPN22 allelic variant. *J. Immunol.* **188**, 487–496 (2012).
51. Shirai, T., Okada, T. & Hirose, S. Genetic regulation of CD5<sup>+</sup> B cells in autoimmune disease and in chronic lymphocytic leukemia. *Ann. NY Acad. Sci.* **651**, 509–526 (1992).
52. Burastero, S.E., Casali, P., Wilder, R.L. & Notkins, A.L. Monoreactive high affinity and polyreactive low affinity rheumatoid factors are produced by CD5<sup>+</sup> B cells from patients with rheumatoid arthritis. *J. Exp. Med.* **168**, 1979–1992 (1988).
53. Thomas, J.W., Kendall, P.L. & Mitchell, H.G. The natural autoantibody repertoire of nonobese diabetic mice is highly active. *J. Immunol.* **169**, 6617–6624 (2002).
54. Kessenbrock, K. *et al.* Netting neutrophils in autoimmune small-vessel vasculitis. *Nat. Med.* **15**, 623–625 (2009).
55. Guiducci, C. *et al.* Autoimmune skin inflammation is dependent on plasmacytoid dendritic cell activation by nucleic acids via TLR7 and TLR9. *J. Exp. Med.* **207**, 2931–2942 (2010).
56. Kono, H. & Rock, K.L. How dying cells alert the immune system to danger. *Nat. Rev. Immunol.* **8**, 279–289 (2008).
57. Hanayama, R. *et al.* Autoimmune disease and impaired uptake of apoptotic cells in MFG-E8-deficient mice. *Science* **304**, 1147–1150 (2004).
58. Todd, J.A. Etiology of type 1 diabetes. *Immunity* **32**, 457–467 (2010).

## ONLINE METHODS

**Mice and treatments.** Female BALB/c, C57BL/6, NOD and *Myd88*<sup>-/-</sup> NOD<sup>59</sup> mice were bred and housed in specific pathogen-free conditions. For pDC and neutrophil depletion, WT NOD mice were injected i.p. on days 14 and 21 after birth, respectively, with 500  $\mu\text{g}$  of depleting m927 mAb per mouse (from M. Colonna) or 250  $\mu\text{g}$  of depleting NIMP-R14 mAb per mouse (from S. Mecheri). For inhibition of IFN- $\alpha$  production by pDCs, WT NOD mice were injected i.p. on days 14 and 21 after birth, with 200  $\mu\text{g}$  of anti-Siglec-H mAb in 200  $\mu\text{L}$  of PBS (ebio440c, eBioscience). The same treatment was performed with respective isotype control. Inhibition of TLR7 and TLR9 was performed using 1  $\mu\text{g}$  per mouse of IRS<sub>954</sub> injected i.p. on days 14 and 21 after birth. TLR9 activation was performed by intravenous injection with 100  $\mu\text{g}$  per mouse of CpG<sub>1585</sub> (Invivogen) on day 14 after birth. For B-1a cell depletion we used a protocol previously described with some modifications<sup>19,60</sup>. Briefly, 1-week-old mice were treated with i.p. injection of 500  $\mu\text{L}$  water every 2 d over 14 d; PBS was injected as negative control. Apoptosis inhibition was performed using Z-VAD (Sigma) as previously described<sup>14</sup>. Mice were injected i.p. with 100  $\mu\text{L}$  per mouse of Z-VAD at 10  $\mu\text{M}$  on days 14 and 21 after birth. Beta cell death was induced by one i.p. injection with 1.6 mg of STZ (Sigma) per mouse. The synthetic mouse cathelicidin peptide CRAMP (Innovagen) was injected i.p. in 4-week-old mice, 200  $\mu\text{g}$  per mouse. This study was approved by the local ethics committee on animal experimentation of Paris Descartes University (CEEA34.JD.046.12).

**Preparation of B-1a cell-conditioned medium.** B-1a cells ( $5 \times 10^3$  in 100  $\mu\text{L}$ ) sorted as CD5<sup>+</sup>CD19<sup>+</sup> cells from pancreatic islets of ten pooled 3-week-old NOD mice were incubated in RPMI complete medium, and cell-free supernatant was recovered after 7 d and stored at  $-80^\circ\text{C}$  before addition to neutrophil or pDC *in vitro* cultures.

**Preparation of plate-bound immune complexes.** Immobilized immune complexes were prepared as follows. Briefly, immune complex-covered surfaces were prepared by incubating 96-well Maxisorp F96 (Nunc International) ELISA plates with 20  $\mu\text{g mL}^{-1}$  genomic dsDNA (Promega) in PBS for 12 h at  $37^\circ\text{C}$ , followed by blocking with 10% BSA in PBS for 1 h and a further 1-h incubation with anti-dsDNA IgG2b mAb (DNA11-M, Genta) at 10  $\mu\text{g/mL}$ . Alternatively, to form B-1a immune complexes, anti-dsDNA IgG2b mAbs were replaced by pancreatic B-1a cell-conditioned medium. Parallel wells prepared without the addition of anti-dsDNA IgGs served as controls.

**Neutrophil stimulation.** Neutrophil activation by immobilized immune complexes (with anti-dsDNA IgG2b mAb) or B-1a immune complexes was achieved by plating the cells on the immune complex-coated surfaces without any additional stimulus. Neutrophils ( $2 \times 10^5$  in 100  $\mu\text{L}$ ) sorted as Ly6G<sup>+</sup> CD11b<sup>+</sup> cells from bone marrow of 3-week-old NOD mice were incubated in complete RPMI. In some conditions, neutrophils were preincubated during 1 h at  $37^\circ\text{C}$  with a mix of blocking anti-Fc $\gamma$ R2/3 (clone 24G2, BD) and anti-Fc $\gamma$ R4 mAbs (clone 9E9, from J. Ravetch) at 10  $\mu\text{g mL}^{-1}$ . Neutrophils were incubated for 20 min for evaluation of CRAMP expression by FACS or for 6 h to generate neutrophil-conditioned medium to stimulate pDCs *in vitro*.

***In vitro* pDC activation by neutrophils and B-1a cells.** Purified splenic pDCs from 3-week-old NOD mice ( $1 \times 10^5$ , Miltenyi kit) were stimulated in 150  $\mu\text{L}$  complete RPMI with neutrophil-conditioned medium (1:3 vol/vol) and/or B-1a cell-conditioned medium (1:3 vol/vol) in the presence or absence of a TLR7/9 inhibitor (IRS<sub>954</sub> 1  $\mu\text{g mL}^{-1}$ ). As a positive control, pDCs were incubated with CpG<sub>1585</sub> (5  $\mu\text{g mL}^{-1}$ ), soluble immune complexes (3  $\mu\text{g/mL}$  dsDNA + 1  $\mu\text{g mL}^{-1}$  anti-dsDNA IgGs, incubated 30 min at room temperature) or CRAMP (50  $\mu\text{g mL}^{-1}$ ). After 36 h of culture, supernatants were recovered and IFN- $\alpha$  production was measured by ELISA (PBL).

**Diabetes diagnosis.** Mice were tested every day for diabetes. Overt diabetes was defined as two positive urine glucose tests, confirmed by a blood sugar level of  $>200$  mg dL<sup>-1</sup>. The Glukotest kit was purchased from Roche.

**Preparation of pancreatic islets.** Mice were killed and pancreata were perfused with 3 mL of a solution of collagenase P (1.5 mg mL<sup>-1</sup>, Roche), then dissected free from surrounding tissues. Pancreata were then digested at  $37^\circ\text{C}$  for 10 min.

Digestion was stopped by adding HBSS-5% FCS followed by extensive washes. Islets were then purified on a discontinuous Ficoll gradient and disrupted adding 1 mL of cell dissociation buffer (GIBCO) for 10 min at  $37^\circ\text{C}$ . After another wash, cells were resuspended, counted and used.

**Flow cytometry.** Cell suspensions were prepared from various tissues and were stained at  $4^\circ\text{C}$  in PBS containing 2% FCS and 0.5% EDTA after Fc $\gamma$ R2/3 blocking. Surface staining was performed with antibodies all from BD Pharmingen or eBioscience (anti-CD11c (clone N418), anti-CD11b (clone M1/70), anti-Ly6G (clone 1A8), anti-CD45 (clone 30-F11), anti-CD19 (clone 1D3), anti-TCR $\beta$  (clone H57-597), anti-CD8 (clone 53-6.7), anti-IFN- $\gamma$  (clone XMG1.2), anti-CD5 (clone 53-7.3), anti-CD21 (clone 8D9), anti-CD1d (clone 1B1)) except m927 mAb and NIMP-R14 mAb, which were conjugated in our laboratory and were used at the concentration of 1  $\mu\text{g mL}^{-1}$ . For CRAMP surface staining, cells were stained sequentially with rabbit anti-CRAMP pAb (from B. Agerberth, 1  $\mu\text{g mL}^{-1}$ ) and anti-rabbit-PE pAb (12-4739-81, eBiosciences, 0.5  $\mu\text{g mL}^{-1}$ ). For intracellular IFN- $\alpha$  staining, the cell suspension was incubated 4 h at  $37^\circ\text{C}$  with Brefeldin A. After fixation and permeabilization (BD Fix&Perm), cells were first stained with anti-IFN- $\alpha$  (clone RMMA-1, 10  $\mu\text{g mL}^{-1}$  PBL); then the surface staining was performed. For NRP-V7 tetramer (from the National Institutes of Health tetramer core facility) staining, cells were stained with tetramers for 45 min at room temperature followed by surface staining for 15 min at  $4^\circ\text{C}$ . Dead cells were excluded using Fixable Viability Dye staining (eBioscience). Stained cells were analyzed and/or sorted on a FACS Aria flow cytometer (BD Biosciences).

**Histology.** Pancreases from NOD mice were collected, embedded in tissue-freezing medium (Jung) and stored at  $-20^\circ\text{C}$ . Tissues were cut into 5- $\mu\text{m}$  sections in a cryostat (Leica). Frozen sections were fixed in cold acetone. Staining with primary antibodies was performed for 1 h with the following antibodies: anti-Ly6G (clone NIMP-R14, from S. Mecheri, 1  $\mu\text{g mL}^{-1}$ ), anti-B220 (clone RA3-6B2, from BD, 1  $\mu\text{g mL}^{-1}$ ) and anti-CD11c-PE (clone N418, from eBiosciences, 1  $\mu\text{g mL}^{-1}$ ) mAbs and insulin (A0564, Dako, 1  $\mu\text{g mL}^{-1}$ ) or CRAMP (from B. Agerberth, 1  $\mu\text{g mL}^{-1}$ ) pAbs. After washing, second-step reagents were applied: anti-rat biotin (A10517, Invitrogen, 1  $\mu\text{g mL}^{-1}$ ) or anti-guinea pig A488 (A11073, Invitrogen, 1  $\mu\text{g mL}^{-1}$ ) pAbs. If necessary, a third-step reagent was applied: streptavidin-PE or streptavidin-APC (eBioscience, 1  $\mu\text{g mL}^{-1}$ ). Nuclei were stained with Hoechst (H1399, Invitrogen, 5  $\mu\text{g mL}^{-1}$ ). Controls with isotype control staining were negative (data not shown).

**Microscopy.** NET production by neutrophils was assessed as follows. Briefly, pancreatic or bone marrow neutrophils were seeded on poly-L-lysine-coated glass (Polysine, Kindler GmbH) at a concentration of  $10^6$  cells per mL for 1 h at  $37^\circ\text{C}$  in RPMI with 2% FCS. Then, cells were stained with anti-Ly-6G-conjugated antibody (clone NIMP-R14) for 10 min on ice and immediately fixed in 2% paraformaldehyde and counterstained for DNA with SYTOX Green (Invitrogen, 100 nM). In some experiments, after fixation, neutrophils were further stained with anti-CRAMP pAb (from B. Agerberth, 1  $\mu\text{g mL}^{-1}$ ) and then counterstained for DNA with SYTOX Green. Slides were analyzed using a Leica TCS SP5 AOBs confocal microscope.

**Quantitative PCR.** Cells were collected in lysis buffer (RLT, Qiagen) buffer with 1% of  $\beta$ -mercaptoethanol. mRNA was isolated using RNeasy Mini Kit (Qiagen) and reverse transcribed with Superscript III (Invitrogen). Quantitative PCR was performed with SYBR Green (Roche) and analyzed with a LightCycler 480 (Roche). Data were normalized to *Gapdh* housekeeping gene.

**Detection of IFN- $\alpha$  or anti-dsDNA IgGs in the pancreatic islets.** Pancreatic islets were recovered by handpicking under a polarized microscope without any prior density separation. Fifty islets from the same mouse were then cultured for 48 h in 100  $\mu\text{L}$  of RPMI complete medium. Supernatants were used for IFN- $\alpha$ -quantification by ELISA (PBL) or for anti-dsDNA IgG quantification by ELISA (Calbiochem).

**Statistical analyses.** Diabetes incidence was plotted according to the Kaplan-Meier method. Incidences between groups were compared with the log-rank test. For other experiments, comparison between means was performed using the non-parametric Mann-Whitney *U*-test. Reported values are means  $\pm$  s.d. as indicated. *P* values  $< 0.05$  were considered statistically significant. All data were analyzed using GraphPad Prism v5 software.

59. Aumeunier, A. *et al.* Systemic Toll-like receptor stimulation suppresses experimental allergic asthma and autoimmune diabetes in NOD mice. *PLoS ONE* **5**, e11484 (2010).

60. Murakami, M., Yoshioka, H., Shirai, T., Tsubata, T. & Honjo, T. Prevention of autoimmune symptoms in autoimmune-prone mice by elimination of B-1 cells. *Int. Immunol.* **7**, 877–882 (1995).

